JOURNAL OF OPTOELECTRONICS AND ADVANCED MATERIALS, Vol. 12, No. 6, June 2010, p. 1327 - 1332

Effect of deposition potential on the physical properties of electrodeposited CuO thin films

T. MAHALINGAM*, V. DHANASEKARAN, G. RAVI, SOONIL LEE[a], J. P. CHU[b], HAN-JO LIM[c]
Department of Physics, Alagappa University, Karaikudi - 630 003, India
[a]*Division of Energy Systems Research, Ajou University, Suwon 442-749, Korea*
[b]*Department of Polymer Engineering, National Taiwan University of Science and Technology, Taipei 10607, Taiwan*
[c]*Department of Electrical and Computer Engineering, Ajou University, Suwon 442-749, Korea*

Semiconducting cupric oxide (CuO) thin films were prepared onto ITO substrates from alkaline medium using electrodeposition technique. CuO thin films were characterized by stylus profilometer, scanning electron microscopy (SEM), X-ray diffraction (XRD) and optical absorption techniques. X-ray diffraction study shows that the electrodeposited CuO thin films are polycrystalline in nature with face centred cubic structure prepared under various deposition potentials. X-ray diffraction studies also reveal that the films exhibit preferential orientation along a (111) plane with crystallite size between 40 and 43 nm. Micro structural properties of films such as lattice parameter, grain size, dislocation density and micro strain were calculated from predominant (111) diffraction lines. The optical constants (refractive index (n) and extinction coefficient (k)) of CuO thin films were evaluated using optical studies. SEM studies show that the grain sizes of CuO thin films vary between 100 and 150 nm and also morphologies revealed that the electrodeposited CuO exhibits uniformity in size and shape. The effect of deposition potential on the physical properties like structure, morphology, microstructure and optical properties of the CuO thin films are studied.

(Received May 28, 2010; accepted June 16, 2010)

Keywords: Electrodeposition, Growth kinetics, CuO thin films, Microstructural parameters, Surface morphology, Structural studies, Optical constants

1. Introduction

In recent years, cupric oxide (CuO) thin films have attracted much interest due to their potential applications in optical and electronic devices. CuO is a p-type semiconductor suitable for applications in solar cells, batteries and field emission devices [1,2]. CuO thin films were prepared using various deposition techniques such as reactive magnetron sputtering [3], spray pyrolysis [4], reactive evaporation [5], RF sputtering [6], Ion beam sputtering [7], plasma evaporation [8], sol-gel [9], molecular beam epitaxy [10], spin coating [11] and electrodeposition [12]. Brijiani et al [13] have prepared Cu_2O thin films by electrodeposition for lithium batteries and studied their characteristics. Kose et al [14] have studied the structural and optical properties of CuO thin films synthesised by spray pyrolysis. Poizot et al [15] reported the electrochemical deposition of CuO from different solution and studied the effects of solution composition and pH on the preparation of the films. Eventhough several reports on the growth and studies of CuO thin films are available, very little work is reported on the influence of deposition parameters such as deposition potential on the properties of electrodeposited CuO thin films. Hence, an attempt is made in the present study to explore the influence of deposition potential on the growth and properties of electrodeposited CuO thin films.

In the present study, we report the preparation of cupric oxide thin films by electrodeposition on indium tin oxide (ITO) coated glass substrates. The thickness, structural, morphological and optical properties of the prepared thin films were obtained using surface profilometer, X-ray diffraction pattern, scanning electron microscopy and optical absorption techniques. Various microstructural parameters are evaluated and the results are discussed.

2. Experimental details

Electrochemical experiments were carried out using a Potentiostat/Galvanostat (EG&G Princeton Applied Research, USA Model 362A). Electrodeposition was performed in a conventional three electrode cell with ITO substrates as cathode and graphite rod as anode and a saturated calomel electrode as reference electrode. CuO thin films were prepared using an electrolyte containing copper sulphate ($CuSO_4$) and L(+) tartaric acid. $CuSO_4$ and tartaric acid were taken with equimolar (30mM) concentrations. Electrodeposition was performed with deposition potential varying from -0.350 V to -0.650 V insteps of 100 mV with respect to SCE. The electrolytic bath temperature and deposition time were maintained at 75^0C and 30 minutes, respectively. Thickness of the deposited films was measured using stylus profilometer (Mitutoyo SJ 301). An X-ray diffractometer [X'PERT

PRO PANalytical, Netherlands] with Cuk$_\alpha$ radiation (λ = 0.1540 nm) was used to identify the crystal structure of the films. Surface morphological analysis was carried out using a scanning electron microscope (Philips Model XL 30, USA). Optical properties of the deposited samples were analyzed using a UV- Vis- NIR double beam spectrophotometer (HR - 2000, M/S ocean optics, USA).

3. Results and discussion

The electrodeposition of CuO thin films was carried out potentiostatically from an alkaline solution bath containing $CuSO_4$ and tartaric acid. The equation is attributed to the formation of Cu^{2+},

$$CuSO_4 \rightarrow Cu^{2+} + SO_4^{2-} (E^0 = 0.34V) \quad (1)$$

Cu^{2+} ions and OH^- ions are generated on the surface of anode and cathode at the same time when direct current passes through the electrochemical cell, and then Cu^{2+} ions react with OH^- ions to produce $CuSO_4$ followed by hydration of $Cu(OH)_2$ to give CuO.

$$SO_4^{2-} + H_2O + 2e \rightarrow 2OH^- + SO_3^{2-} (E^0 = -0.94V) \quad (2)$$

$$Cu^{2+} + 2OH^- \rightarrow Cu(OH)_2 \quad (3)$$

$$Cu(OH)_2 \rightarrow Cu^{2+} + 2OH^- \quad (4)$$

Equation (4) leads to the formation CuO thin films by electrodeposition technique. In this reaction the tartarate ions induce the separation of $CuSO_4$ molecules from meta-stable state to yield cupric oxide at pH 13.0. Finally, cupric oxide film is obtained by the reaction,

$$Cu^{2+} + 2OH^- \rightarrow CuO + H_2O \quad (5)$$

CuO thin films were prepared at various deposition potentials ranging from -350mV to -650mV vs SCE by maintaining the deposition time and bath temperature at 30 minutes and 75^{0}C, respectively. The structural properties of electrodeposited CuO thin films was investigated by X-ray diffraction using Cuk$_\alpha$ radiation with λ = 0.154nm. X-ray diffraction patterns are recorded for CuO thin films obtained at different deposition potentials. Typical X-ray diffraction pattern of as-deposited CuO films are shown in figure 1. X-ray diffraction studies revealed that as-deposited films were polycrystalline nature. X-ray diffraction patterns also show that various diffraction peaks at 2θ values 35.25^0, 36.43^0, 61.340 and 74.11^0, were identified to originate from (-111) (111) (220) and (222) planes, respectively, which corresponds to CuO face centred cubic phase. The observed peaks in the diffraction patterns were indexed and the corresponding values of lattice spacing "d" were calculated and compared with JCPDS standards [16]. X-ray diffraction patterns also revealed that the films exhibited a preferential orientation along (111) plane. The preferred orientation of the CuO films can be controlled by adjusting the deposition potential. Fig. 1 indicates that the intensity and broadening of the peak (111) increase with decrease in the deposition potential. This indicates that the grain size along (111) plane and the crystallinity decrease as the deposition potential becomes more negative.

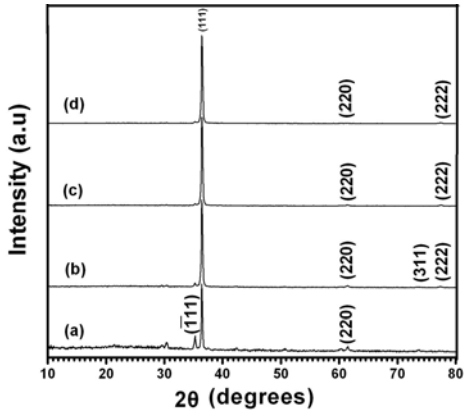

Fig. 1 X-ray diffraction patterns of typical CuO thin films deposited at various potentials (a) -350 mV vs SCE (b) -450 mV vs SCE (c) -550 mV vs SCE and (d) -650 mV vs SCE.

The variation of CuO film thickness with deposition potential is represented in Fig. 2. The film thickness gradually increases with increase of deposition potential and it is attributed to the increase in deposition rate. Film thickness is found to influence microstructural [17] and optical properties [14]. In microelectronic applications, the film thickness is to be scaled down to the device size. Therefore, it is valuable to examine how CuO microstructure evolves with thickness and hence the resulting physical properties. It is observed that the film thickness gradually increases with deposition potential when other parameters such as bath temperature and deposition time are kept constant.

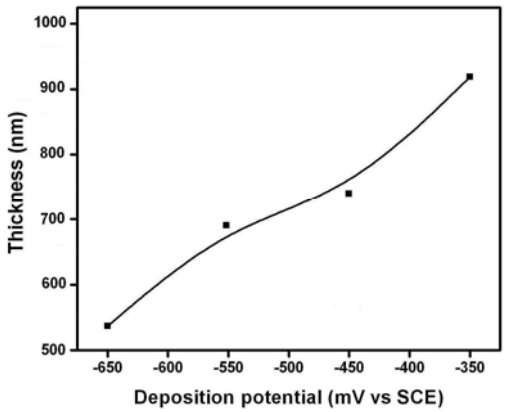

Fig. 2 Thickness variation versus deposition potential of electrodeposited CuO thin films

The crystallite size D of the films was calculated from the Debye Scherer's formula from the full-width at half-maximum intensity (FWHM) expressed in radians D=[0.9λ/βcosθ], where D is crystallite size and β is the FWHM. From (hkl) planes, the lattice constants were evaluated using the relation, $d = [a * (h^2+k^2+l^2)^{-1/2}]$ where d is the inter planar spacing of the atomic plane. The variation of crystallite size and lattice constant with deposition potential is shown in figure 3a and 3b. The crystallite size can be controlled simply by varying the applied potential. The crystallite sizes are in the range between 40 and 43.2 nm for films deposited at potentials ranging from -350mV to -650mV versus SCE. The crystallite size is found to decrease gradually with increase in deposition potential from -650 mV to -350 mV versus SCE. A dramatic decrease in crystallite size has been observed in these (111) oriented films when the applied potential changes from -650 mV towards -350 mV vs SCE as shown in figure. 3. We attribute the decrease in the crystallite size to the increase of deposition rate. Since the change of applied potential from -650 mV towards -350 mV vs SCE corresponds to the increase of steady-state current, which results in the increase of deposition rate. The decrease of crystallite size with the increase of deposition rate has been observed in previous work by Matsomoto [18] and Zhou [19]. Initially, the lattice constant increases slowly with deposition potential and when the deposition potential is increased above -550mV vs SCE, there is a rapid increase in the lattice constant shown in Fig. 3. This suggests that crystallinity and preferential orientation increases with increasing deposition potential.

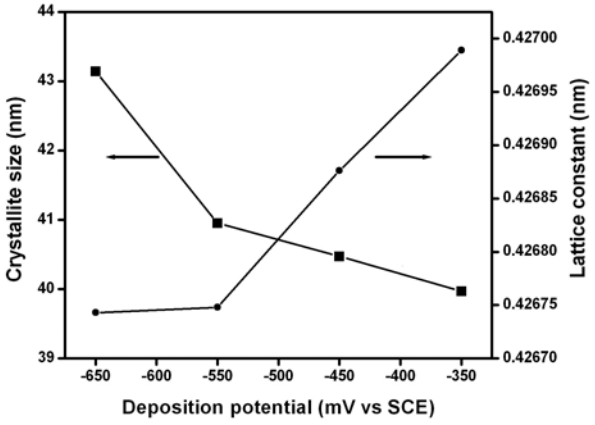

Fig. 3 Crystallite size and lattice constant of the CuO thin films versus various deposition potential

The microstrain and dislocation density for the electrodeposited CuO films were obtained from full width at half maximum which can be expressed as linear combination of contributes from the particle size, D and strain ε given below. The origin of the micro strain is related to the lattice misfit, which in turn depends upon the deposition conditions. The micro strain ε is calculated using the relation,

$$\frac{\beta\cos\theta}{\lambda} = \frac{1}{D} + \frac{\varepsilon\sin\theta}{\lambda} \tag{6}$$

where λ is wavelength, D is crystallite size, β is FWHM of the predominant orientation and θ is Bragg's angle. The dislocation density δ defined as the length of dislocation lines per unit volume of the crystal and can be evaluated from the particle size D by the relation:

$$\delta = \frac{n}{D^2} \tag{7}$$

where n is a factor, when equal unity giving minimum dislocation density. Figs. 4a and 4b represent the dislocation density (δ) and the microstrain (ε) of CuO thin films electrodeposited with different deposition potentials. Microstrain and dislocation density are increasing with increase in deposition potential. The maximum value of microstrain and dislocation density are found to be 6.3 x 10^{14} lines/m^2 and 2.0 x 10^{-3} m, respectively, for the film deposited at -350mV vs SCE.

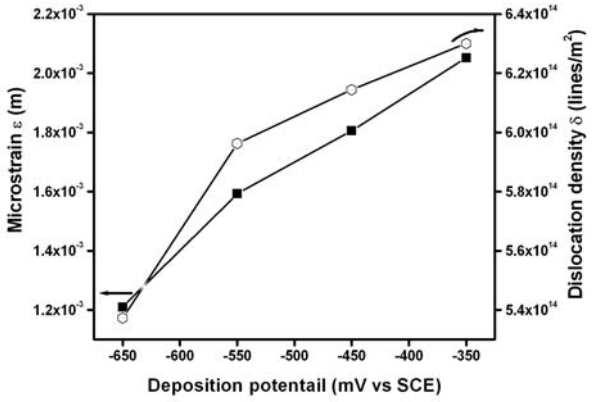

Fig. 4 Microstrain and dislocation density of the CuO thin films versus various deposition potential

The number of crystallites per unit area (N) of the films was determined with the using formula,

$$N = \frac{t}{D^3} \tag{8}$$

where t is thickness of the film, N number of crystallites per unit area and D crystallite size. The number of crystallites per unit area is found to rapidly increase with increase in deposition potential from -650mV to -550 mV versus SCE. Further increase of deposition potential leads to gradual increase in the number of crystallites per unit area which may be attributed to the reduction in crystallite size with increase in deposition potential shown in figure

5. The texture coefficient was calculated using an expression

$$P(h_i k_i l_i) = \frac{I(h_i k_i l_i)}{I_0(h_i k_i l_i)} \left[\frac{1}{n} \Sigma \frac{I(h_i k_i l_i)}{I_0(h_i k_i l_i)} \right]^{-1} \quad (9)$$

where I_0 represents the standard intensity, I is the observed intensity of $(h_i k_i l_i)$ plane and n is the reflection number. The crystallite shape of the CuO film is strongly related to the texture of CuO film. The texture coefficient of different lattice planes of CuO thin films are shown in figure 5. The predominant plane orientation of the film has high texture coefficient value. The variation of texture coefficient of CuO thin films with deposition potential along various crystallographic planes such as (-111), (111), (220) and (222) are shown in Fig. 5. The texture coefficient is found to be higher for the predominant plane (111) than for other planes such as (220) and (221). Also, the texture coefficient along (111) plane is found to be decreasing with increase in deposition potential. It has been reported for copper oxide film [14] earlier that texture coefficient is higher than 1 indicates preferential orientation and also indicates the abundance of grains in a given (h_i,k_i,l_i) direction. It is found that the texture coefficient is maximum for all the peaks of films deposited at -650mV vs SCE and as the deposition potential increase, the texture coefficient decreases. The texture coefficient for the predominant peak (111) is found to be 3.7 for the film deposited at -650mV vs SCE.

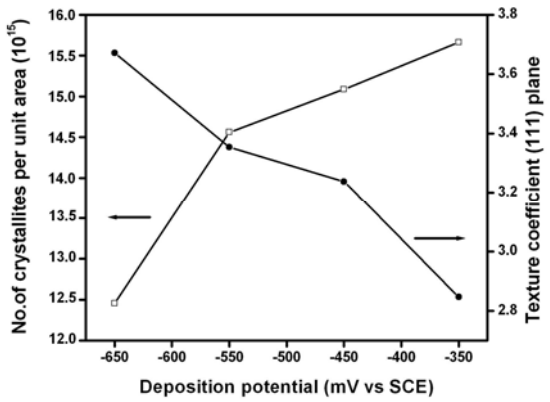

Fig. 5. Number of crystallite per unit area and texture coefficient (111) plane of the CuO thin films versus various deposition potential.

Optical transmission spectra were recorded at room temperature in air to obtain information on the optical properties of cupric oxide thin films. Refractive index (n) and extinction coefficient (k) of cupric oxide films are estimated using the expressions [20],

$$n = \frac{1+R}{1-R} + \sqrt{\frac{4R}{(1-R)^2} - k^2} \quad (10)$$

$$k = \frac{\alpha\lambda}{4\pi} \quad (11)$$

where α is absorption coefficient, λ is wave length and R is reflectance of the CuO thin films. The refractive index and extinction coefficient of the thin films are estimated from following equations (10) and (11). The refractive index and the extinction coefficient spectra of CuO thin films are shown in Figs. 6 and 7. It was observed from these figures 6 and 7 that the refractive index decreases with deposition potential, while the extinction coefficient increases for electrodeposited CuO thin films. The value for the refractive index lies between 2.590 and 2.725 and value of extinction coefficient lies between 0.025 and 0.01. It is also seen in figure that the refractive index significantly changes with thickness of the films. It is evaluated that in the refractive index spectra, the lower thickness films exhibit a higher energy region, while the higher thickness films exhibit a lower energy region.

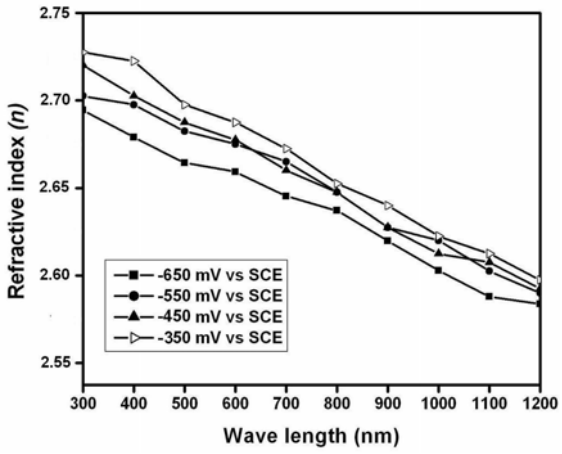

Fig. 6 Refractive index spectra of electrodeposited CuO thin films.

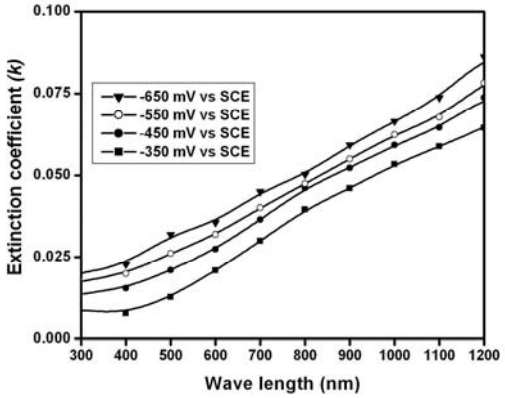

Fig. 7. Extinction coefficient spectra of electrodeposited CuO thin films.

The optical parameters such as absorption coefficient and band gap are determined from optical absorption measurements. The value of absorption coefficient for strong absorption region of thin film is calculated using the following equation (12) [21],

$$\alpha = \frac{1}{t}\ln\left(\frac{A}{T}\right) \tag{12}$$

where α is the absorption coefficient in cm^{-1}, t is the thickness of the films, A is absorbance and T is transmittance. The nature of transition is determined using the following equation (13) [22],

$$\alpha h\nu = A\left(h\nu - E_g\right)^n \tag{13}$$

where α is absorption coefficient in cm^{-1} , hν is photon energy, Eg is an energy gap, A is energy dependent constant and n is an integer. The optical band gap of CuO thin films deposited at various potentials were estimated using optical absorption data derived from optical measurements. The band values are obtained by extrapolating the linear portions of the plots (hν) versus $(\alpha h\nu)^{1/2}$ to the energy axis. It is observed that electrodeposited CuO thin films exhibit indirect transition. CuO thin films with an indirect band gap were reported earlier [23]. The band gap values are estimated to be varying between 1.45 eV and 1.51 eV and it is also observed that band gaps are found to increase with increase of deposition potential showing the effect of deposition potential on the optical band gap. The differential transmittance method has been used and the results are verified and included inset to figure 8. Kazuyuki et al [24] have reported that their electrodeposited CuO thin films revealed a similar deposition current density dependence on the band gap.

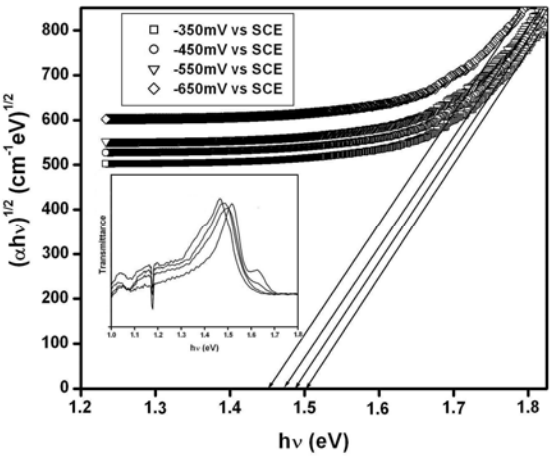

Fig. 8 Plots of energy versus $(\alpha h\nu)^{1/2}$ and inset figure shows band gap value estimated using differential transmittance method.

The surface morphology of electrodeposited CuO thin film was investigated using a scanning electron microscope. The grain sizes of the films are found to increase with decrease in deposition potential. Figure 9a shows the typical SEM micrograph obtained for CuO film deposited at -350 mV vs SCE. From figure 9a it is seen that the grain boundary could not be obviously observed on the surfaces, but the micrographs reveal various types of distribution of the particles on the film surface depending on the deposition potential. It is observed that the film surface constitutes inhomogeneous mixer of needle like and spherical grains. The reason for this state may be attributed to the tense state of the surface of the films. The compression of spherical grains to yield needle like elongate ellipsoidal grains may be due to the inability to find the grain boundaries by the usually formed spherical grains.

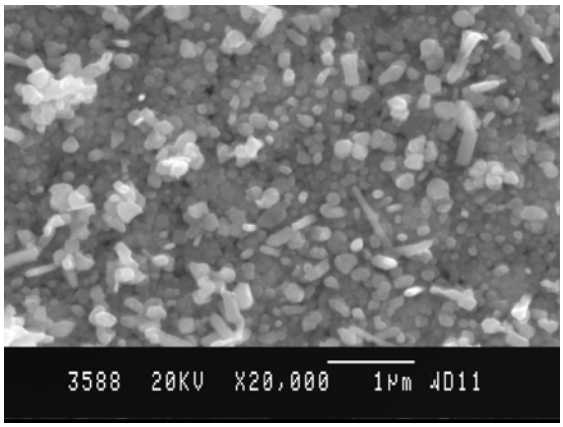

Fig. 9(a) SEM picture of the electrodeposited CuO thin film at a deposition potential -350 mV vs SCE.

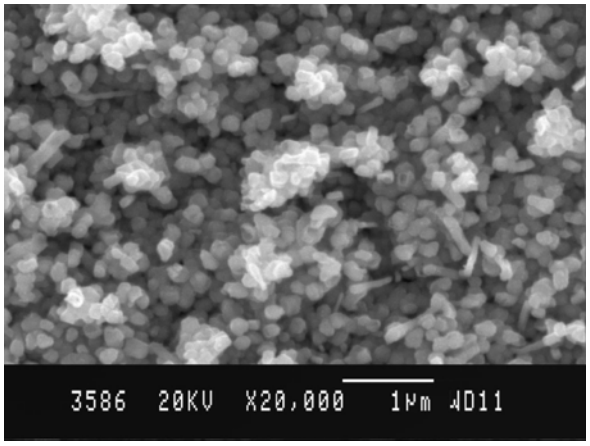

Fig. 9(b) SEM picture of the electrodeposited CuO thin film at a deposition potential -650 mV vs SCE.

However, in figure 9b the SEM micrograph obtained at less deposition potential (-650 mV vs SCE) reveals a surface uniformly constituted. It is observed in figure 9b that the surface homogeneity of the films is improved. It is also observed that small grains agglomerate to form larger grains. The surface is covered well with more number of spherical grains. The grain sizes of CuO thin film covered the entire surface of the film are estimated to be in the range between 80 and 120 nm. When the deposition potential is decreased to -650 mV vs SCE, more grain growth occur, thereby the average grain size is increased due to agglomeration of smaller grains together. The grains tend to agglomerate and the tension may be comparatively less is the surface of the films with the number of needle like ellipsoidal grains are less. It is evident that by altering the deposition potential the surface features may be modified. When the deposition potential is decreased, the surface mobility is increased. This is turn allows the films to lower its total energy by grain growth and decrease in the grain boundary areas.

4. Conclusion

Cathodic deposition of CuO thin films on tin oxide coated glass substrates was carried out potentiostatically under various deposition potentials. The applied potential has been found to have significant effect on the structural, morphological and optical properties of CuO thin films. The microstructural parameters for CuO thin films were evaluated and found to depend on the deposition potential. The increase of deposition potential is found to yield CuO thin films with lower crystallite size. The surface morphology reveals uniform grains for films deposited at deposition potential -650 mV vs SCE. The band gap of CuO films obtained in this work is quite closer to the value reported earlier. The optical constants of CuO thin films are also found to be sensitive to changes in deposition potential. It was observed that the refractive index (n) decreases and extinction coefficient (k) increases, with increase in deposition potential.

References

[1] K. Akimoto, S. Ishizuka, M. Yanagita, Y. Nawa, G. K. Paul, T. Sakurai Solar Energy **80**(6), 715 (2006).
[2] S. S. Jeong, A. Mittiga, E. Salza, A. Masci, S. Passerini Electrochim. Acta **53**(5), 2226 (2008).
[3] A. H. Jayatissa, K. Guo, A. C. Jayasuriya Applied Surface Science **255**(23), 9474 (2009).
[4] J. Morales, L. Sánchez, F. Martín, J.R. Ramos-Barrado, M. Sanchez Electrochim. Acta **49**, 4589 (2004).
[5] B. Balamurugan, B.R. Mehta Thin Solid Films **396**, 90 (2001).
[6] S. Ghosh, D.K. Avasthi, P. Shah, V. Ganesan, A. Gupta, D. Sarangi, R. Bhattacharaya, W. Assmann Vacuum, **57**, 377 (2000)
[7] K. H. Yoon,W. J. Choi, D. H. Kang, Thin Solid Films **372**, 250 (2000).
[8] K. Santra, C. K. Sarker, M.K. Mukherjee, B. Ghosh, Thin Solid Films **213**, 226 (1992).
[9] A. Y. Oral, E. Mensur, M. H. Aslan, E. Basaran, J. Mat. Chem. And Phy. **83**(1), 140 (2004).
[10] K. P. Muthe, J. C. Vyas, S. N. Narang, D. K. Aswal, S. K. Gupta, D. Bhattacharya, R. Pinto, G. P. Kothiyal, S. C. Sabharwal Thin Solid Films **324**, 37 (1998).
[11] M. A. Brookshier, C. C. Chusuei, D. W. Goodman, Langmuir **15**, 2043 (1999).
[12] E. W. Bohannan, I. M. Nicic, H. M. Kothari, J. A. Switzer Electrochim. Acta **53**, 155 (2007).
[13] S. Bijani, M. Gabas, L. Martinez, J. R. Ramos-Barrado, J. Morales, L. Sanchez, Thin Solid Films **515**, 5505 (2007).
[14] S. Kose, F. Atay, V. Bilgin, I Akyuz, J. Mat. Chem. And Phy. **111**, 351 (2008).
[15] P. Poizot, C. J. Hung, M. P. Nikiforov, E. W. Bohannan, J. A. Switzer, Electrochem. Solid-State Lett. **6**(2), C21 (2003)
[16] JCPDS card No. 78-0428, 2003
[17] S. B. Qadri, E. F. Skelton, D. Hsu, A. D. Dinsmore, J. Yang, H. F. Gray, B. R. Rata, Phys. Rev. B **60**, 9191 (1999)
[18] Y. Matsumoto, J. Hombo, C. Qiong, J. Electroanal. Chem. **279**, 331(1990)
[19] Y. C. Zhou, R. J. Phillips, J. A. Switzer, J. Am. Ceram. Soc. **78**, 981 (1995)
[20] N. Benramdane,W. A. Murad, R. H.Misho, M. Ziane, Z. Kebbab, J. Mat. Chem. And Phy. **48**, 119 (1997).
[21] J. C. Manitacier, J. Casiot, P. Fillard, J. Phys. E **9,** 1002 (1976).
[22] S. Thanikaikarasan, T. Mahalingam, M. Raja, Taekyu Kim, Y. D. Kim, J. Mater. Sci. Mater. Electron **20**, 727 (2009).
[23] M. J. Siegfried, K. S. Choi, J. Electrochem. Soc. **154**(12), D674 (2007).
[24] T. Kazuyuki, S. Junji, T. Toshihide, M. Izaki, I. Mitsuteru ECS Meeting Abstracts **802**, 125 (2008).

*Corresponding author: maha51@rediffmail.com